NEDC-23702
Class I
March, 1978

MARK I CONTAINMENT SEISMIC SLOSH EVALUATION

MARK I CONTAINMENT PROGRAM, TASK 5.4

S. M. Arain

Approved: W. J. McConaghy
W. J. McConaghy, Manager
Generic Containment Programs

Approved: G. E. Wade
G. E. Wade, Manager
Mark I Containment
Design

Approved: P. W. Ianni
P. W. Ianni, Manager
Containment Design

NUCLEAR ENERGY ENGINEERING DIVISION • GENERAL ELECTRIC COMPANY
SAN JOSE, CALIFORNIA 95125

GENERAL ELECTRIC

DISCLAIMER OF RESPONSIBILITY

This document was prepared by or for the General Electric Company. Neither the General Electric Company nor any of the contributors to this document:

A. Makes any warranty or representation, express or implied, with respect to the accuracy, completeness, or usefulness of the information contained in this document, or that the use of any information disclosed in this document may not infringe privately owned rights; or

B. Assumes any responsibility for liability or damage of any kind which may result from the use of any information disclosed in this document.

TABLE OF CONTENTS

LIST OF ILLUSTRATIONS

LIST OF TABLES

ABSTRACT

An analytical study and 1/30 scale model tests of the Mark I torus were conducted to determine seismically induced slosh amplitudes and slosh pressures. Twenty-one seismic tests were performed to investigate the sensitivity of the pool response to the various earthquake acceleration intensities along horizontal and vertical axes. The tests enveloped the range of Mark I Final Safety Analysis Report (FSAR) seismic criteria. An analytical model, calibrated with the test results, was developed for calculating these Mark I seismic slosh responses. The results show that the downcomers of the Mark I plants will remain submerged if a slosh is generated by a Safe Shutdown Earthquake (SSE). The calculated slosh pressures on torus walls of the Mark I plants were found to be insignificant.

ACKNOWLEDGEMENTS

This report is based upon the work of Dr. D. D. Kana and Dr. J. F. Unruh at Southwest Research Institute, San Antonio, Texas, under contract to General Electric Company.

1. INTRODUCTION

An analytical and experimental investigation of the Mark I torus was conducted to determine seismically induced slosh amplitudes and slosh pressures. The specific objectives of the program were to:

1. Determine the slosh amplitudes at the downcomers and at the torus walls.

2. Determine the maximum slosh pressures on the torus walls.

3. Provide an analytical model capable of generating seismic slosh results for the Mark I plants.

Details of the experimental and analytical programs together with the results achieved are described in this report.

A 1/30 scale torus model, made of Plexiglas, was constructed complete with vent header, downcomer, ring girders and mitre joints. The scaling criteria of the model were based on the scaling analysis described in the "Mark III Containment Seismic Slosh" report (Reference 1), and in the "Dynamic Behavior of Liquids in Moving Containers" report (Reference 2). The model was tested on a seismic shake table by subjecting it to simulated earthquakes covering the range of Mark I design values. Transducers were mounted at various locations in the model to measure slosh pressures and slosh amplitudes as a function of time. Motion pictures were taken to provide a visual record of the seismically induced slosh.

An analytical model, which simulates the pressure suppression chamber, is provided to generate seismic slosh results for the individual Mark I plant geometries. The model was calibrated with the test results of the 1/30 scale model.

2. SUMMARY OF RESULTS

2.1 SEISMICALLY INDUCED SLOSH

The Mark I seismic slosh tests, performed with the envelope of the Mark I FSAR seismic criteria (see Section 2.3) have clearly demonstrated that the downcomer vents will remain submerged in the event of slosh caused by a Safe Shutdown Earthquake (SSE). The calculated slosh amplitudes for the full scale Mark I plants are small, as shown in Table 2-1 below. These results are conservative since the seismic response spectrum used in the seismic slosh tests is an envelope of the individual response spectra for all the Mark I plants and the results are modified for one-sided 95-95 percent statistical tolerance limit (see Section 5.1.1).

Table 2-1
MARK I CONTAINMENTS SEISMIC SLOSH RESULTS[a]

Plant	Slosh Amplitudes (inches)[b] Inner Wall (η_{IW})	Inner Downcomer (η_{ID})	Outer Downcomer (η_{OD})	Outer Wall (η_{OW})	Minimum Downcomer Submergence (inches)**
Brown's Ferry 1,2,3	21.0	10.4	11.3	13.5	50.0
Brunswick 1, 2	15.5	7.8	8.5	10.0	48.0
Cooper	19.8	10.3	11.1	12.6	48.5
Dresden 2,3	21.2	10.7	11.7	13.6	44.0
Duane Arnold	11.2	2.2	*	7.3	47.5
Fermi 2	16.7	8.3	9.0	10.8	48.0
Fitzpatrick	15.5	7.9	8.6	10.0	50.0
Hatch 1, 2	14.9	7.7	8.5	9.7	44.0
Millstone	16.4	8.4	8.9	10.4	57.0
Monticello	11.1	5.9	6.3	7.1	54.5
Nine Mile Point	10.2	4.3	4.6	6.9	36.0
Oyster Creek	20.7	9.6	9.9	13.0	52.8
Peach Bottom 2,3	12.6	6.2	6.7	8.1	48.0
Pilgrim	14.3	7.3	7.7	9.1	45.0
Quad Cities 1,2	25.0	12.6	13.7	16.1	38.5
Vermont Yankee	12.9	6.8	7.3	8.2	51.5
Hope Creek	20.8	10.3	11.1	13.4	48.0

a. Based on SSE Envelope Spectrum (see Appendix B for definition of envelope spectrum).

b. Includes Global Correction Factor modified for one-sided 95-95 percent statistical tolerance limit for each parameter given in Table 5-4.

* Single Downcomer on vent header vertical centerline.

** Values as of March, 1978.

2.2 PEAK WALL PRESSURES

The magnitude of the maximum calculated local slosh pressures on the full scale torus wall were found to be small (≤ 0.43 psi at statistical mean and ≤ 0.69 psi at one-sided 95-95 percent statistical tolerance limit).

2.3 SEISMIC DRIVING CONDITIONS

The seismic criteria used for this investigation are given in Appendix B. The seismic response spectrum envelopes shown in Figure B-1 of Appendix B were obtained by geometrically enveloping the individual response spectra for each of the Mark I plants. The simulated earthquake time histories for the tests were developed based on the envelope response spectrum. The seismic input level of the tests ranged from the Operating Basis Earthquake (OBE) to twice the level of the Safe Shutdown Earthquake (2 SSE).

2.4 ANALYTICAL MODEL

A simple analytical model, based on Mark III suppression pool type annular tank geometry, was used to calculate the Mark I seismic slosh response. The model was developed in the Mark III containment seismic slosh study (Reference 1). The test results for slosh amplitudes, pressures and downcomer moments were found to be higher than those predicted by the analytical model. Differences in all cases between the analytical and experimental results were eliminated by the introduction of global correction factors and harmonic correction factors. The global correction factor is a direct multiplier of the magnitude of the calculated slosh parameter from the analytical model. The harmonic correction factor is a direct multiplier of each of the magnitudes of the first three modes of predicted slosh response for each parameter from the analytical model. The harmonic correction factor is incorporated into the analytical model before the global correction factor is applied. The analytical model modified with both of these factors provides results in agreement with the experimental data for slosh amplitudes, slosh pressures, and downcomer moments. The modified analytical model with one-sided 95-95 percent statistical tolerance limit for the slosh amplitude response was used in predicting the corresponding response of full-scale Mark I plants in Table 2-1.

3. TEST DESCRIPTION

3.1 TEST FACILITY

A 1/30 scale Plexiglas model of the Mark I torus (Figure 3-1) was built to evaluate seismic slosh in the suppression pool. Pertinent parameters for the referenced Mark I torus system are given in Figure 3-2 for both the prototype and the 1/30 scale model, and a sketch of the first three slosh modes is shown in Figure 3-3. The scaling bases for developing the model parameters were taken from Reference 1 and are summarized in Table 3-1. Figures 3-4 through 3-6 show details of the scale model, which was a torus formed by bonding together 16 straight tubular sections. The torus model was designed for separation into upper and lower segments at the inner and outer flanges to enhance installation of instrumentation and a vent header/downcomer assembly. A portion of the torus was designed without a flange at the major diameter to improve visual observation of slosh and to facilitate an unobstructed view for a movie camera to obtain film records of the tests.

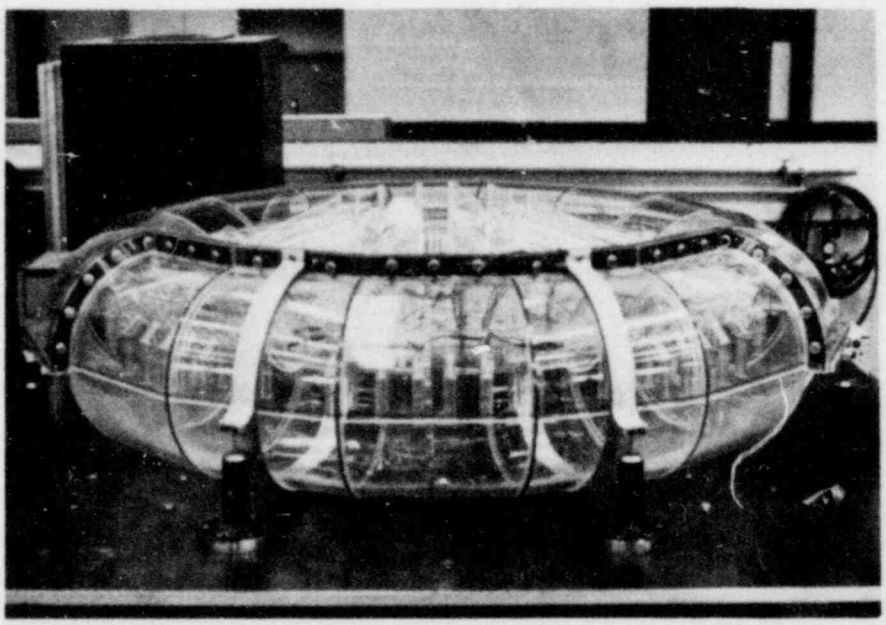

Figure 3-1
1/30 Scale Model of Mark I Torus System

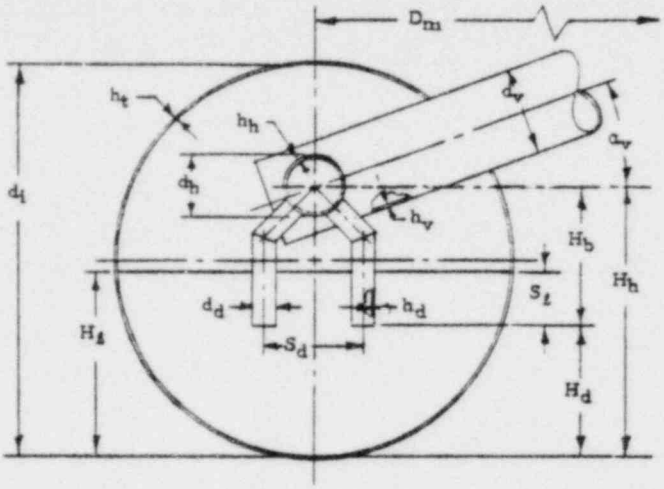

Symbol	Parameter Identification	Prototype	Model
D_m	Torus Mean Diameter	111.00 ft.	44.40 in.
d_t	Section Inner Diameter	31.00 ft.	12.40 in.
d_h	Header Outer Diameter	4.84 ft.	2.00* in.
d_v	Vent Outer Diameter	6.83 ft.	2.75* in.
d_d	Downcomer Outer Diameter	2.00 ft.	0.75* in.
H_t	Liquid Level	14.67 ft.	5.87 in.
H_h	Header Centerline Level	21.35 ft.	8.54 in.
H_d	Downcomer Level	10.47 ft.	4.18 in.
H_b	Downcomer Vertical Length	10.88 ft.	4.35 in.
h_t	Torus Wall Thickness	0.75 in.	0.50* in.
h_h	Header Wall Thickness	0.50 in.	0.12* in.
h_d	Downcomer Wall Thickness	0.020 in.	0.12* in.
h_v	Vent Wall Thickness	0.50 in.	0.12* in.
S_d	Downcomer Mean Separation	8.00 ft.	3.20 in.
S_t	Downcomer Submergence	4.26 ft.	1.70 in.
α_v	Vent Angle to Horizontal	20°	20°
f_{t1}	First (m = 1, n = 1) Slosh Mode	0.055 Hz	0.301 Hz
f_{t2}	Second (m = 1, n = 2) Slosh Mode	0.268 Hz	1.468 Hz
f_{t3}	Third (m = 1, n = 3) Slosh Mode	0.403 Hz	2.207 Hz
f_{sr}	Rigid Support Mode	33.5 Hz	183.49 Hz
f_{sm}	Medium Support Mode	6.0 Hz	32.86 Hz
f_{sf}	Flexible Support Mode	2.7 Hz	14.79 Hz
ζ_s	Support Mode Damping	2%	2%

* Denotes slightly distorted scale

Figure 3-2
Mark I Torus Parameters for Model and Reference Plant Prototype
(GE Company Proprietary)

Table 3-1

SUMMARY OF VARIABLES AND SCALING FACTORS FOR 1/N SCALE MODEL OF MARK I SUPPRESSION POOL

Variable	Prototype	Model
Tank		
Tank Dimension	ℓ_p	ℓ_p/N
Excitation		
Tank Base Absolute Acceleration	a_{1H}, a_{1V}	a_{1H}, a_{1V}
Frequency	ω_p	$N\ \omega_p$
Tank Base Pseudo Relative Displacement	$(X_{1H})_p$, $(X_{1V})_p$	$(X_{1H})_p/N$, $(X_{1V})_p/N$
Tank Base Pseudo Relative Velocity	$(X_{1H}\omega)_p$, $(X_{1V}\omega)_p$	$(X_{1H}\omega)_p/\sqrt{N}$, $(X_{1V}\omega)_p/\sqrt{N}$
Earthquake Duration	$(T_e)_p$	$(T_e)_p\ \sqrt{N}$
Liquid		
Depth	H_p	H_p/N
Damping	ζ_p	ζ_p
Displacement	η_p	(η_p/N)
Pressure	p_p	p_p/N
Downcomer Moment	M_p	M_p/N^4

NOTE: Use of identical liquid density (ρ_ℓ) and gravity field (g) is assumed in this correlation.

Company Proprietary

Figure 3-3
First Three Slosh Modes in 1/30 Scale Model Torus
(GE Company Proprietary)

The vent tubes, vent header, and downcomer tubes were all fabricated from plastic tube sections which were bonded together. The assembly of eight vent tubes, vent header and downcomer system is shown in Figures 3-4 and 3-5. The vent tubes that extended into the torus through individual clearance holes were supported on a flat aluminum plate, which provided rigidity relative to the table and maintained proper alignment for the assembly. Thus, the header system was designed to be rigid, with respect to the shake table, both horizontally and vertically.

The torus model was supported on 16 posts of adjustable length, representing dynamically modeled supports, as shown in Figure 3-7. The purpose of this arrangement was to evaluate the influence of support conditions on the slosh amplitudes and loads. The testing was performed under three different support conditions -- rigid, medium, and flexible -- representing the range of selected frequencies listed in Figure 3-2. The support conditions were obtained by adjusting the lengths of the support posts to match the desired frequencies.

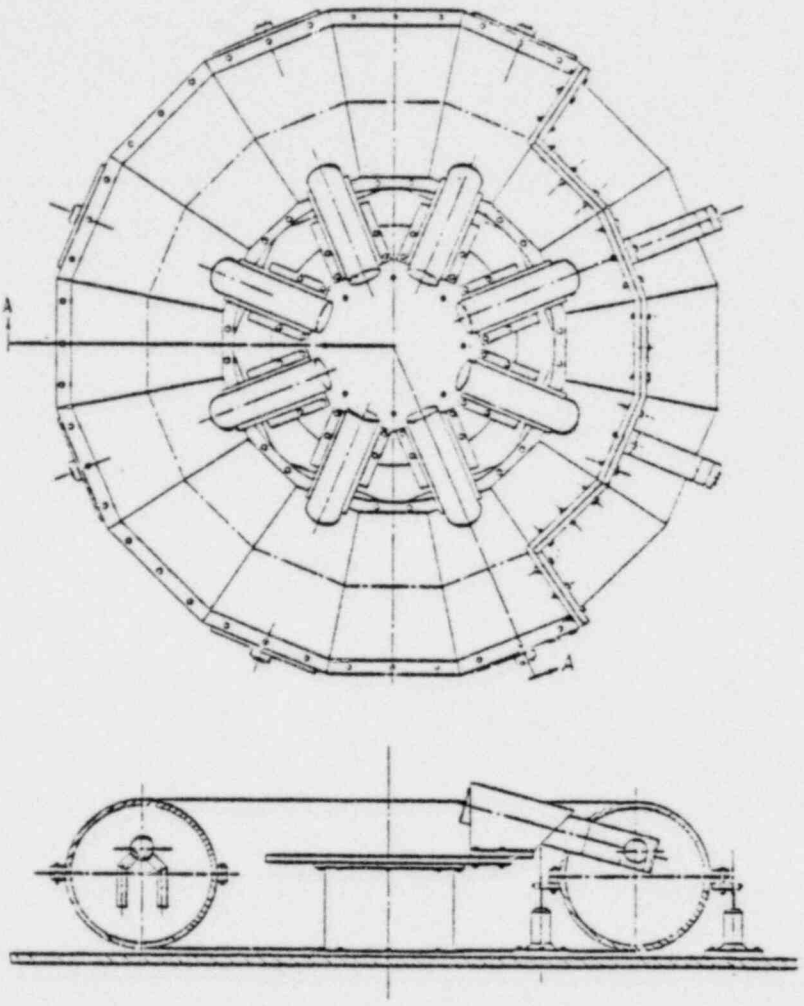

Figure 3-4
General Design of Mark I Torus 1/30 Scale Seismic Model

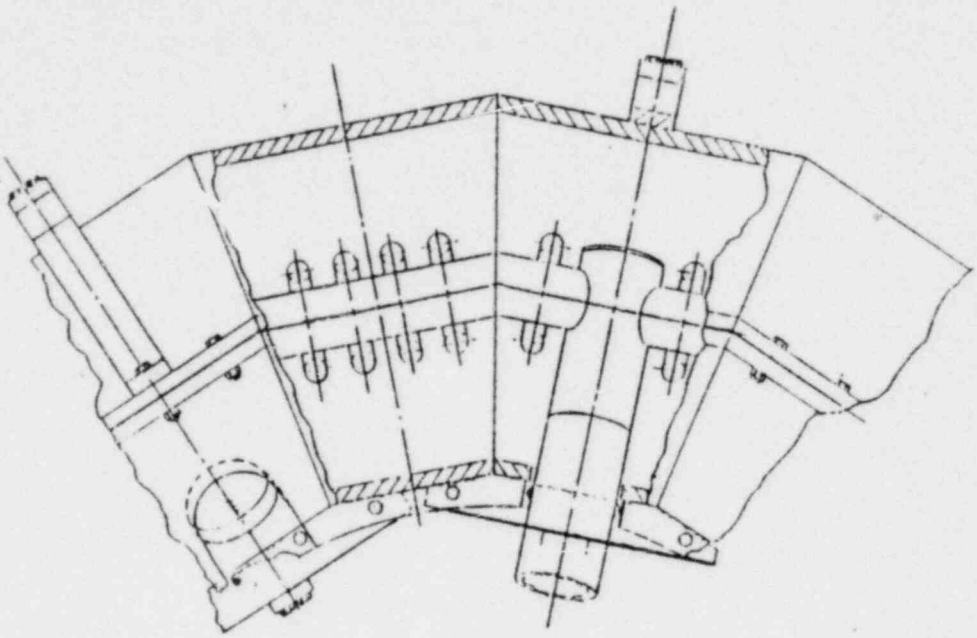

Figure 3-5
Plan View of Torus and Internals

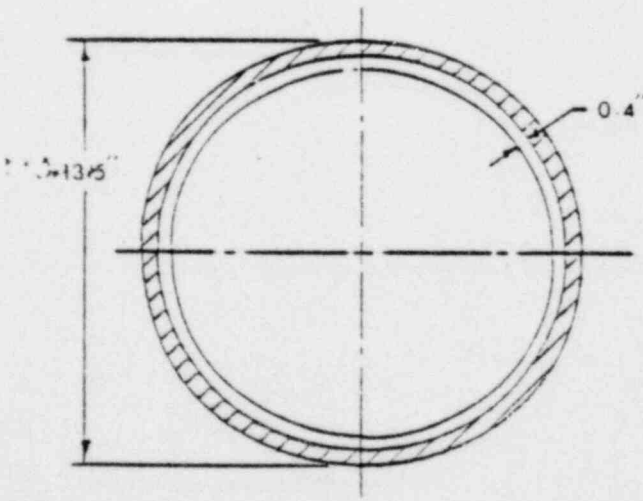

Figure 3-6
Simulated Ring Girder

3.2 INSTRUMENTATION

The instrumentation arrangement is shown in Figures 3-7 and 3-8. Twenty-two channels of data were recorded on the FM analog tape recording system, using a single 14-channel tape recorder. This was done by repeating the test runs for each test with altered channel distribution. Several reference data channel allocations were maintained to ensure that identical excitation conditions were used for both test runs. Tables 3-2 and 3-3 list the parameters along with their corresponding symbols and tape recorder channels.

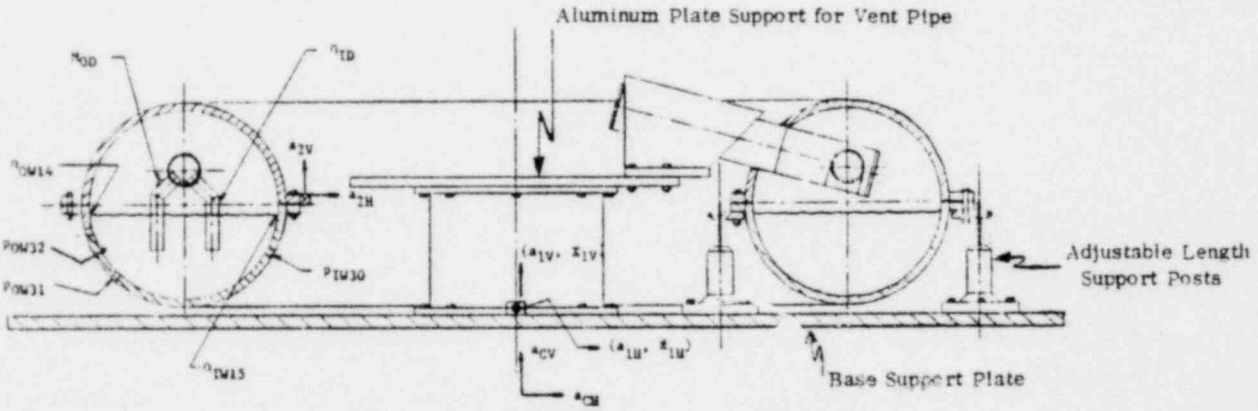

a_{CH}, a_{CV}	- Command Accelerations	P_{IW30}	- Innerwall Pressure
a_{1H}, a_{1V}	- Control Accelerations	M_{OD}, M_{ID}	- Downcomer Moments
X_{1H}, X_{1V}	- Control Displacements	η_{OW}, η_{IW}	- Tank Wall Wave Heights
a_{2H}, a_{2V}	- Tank Accelerations	η_{OD}, η_{ID}	- Downcomer Wave Heights
P_{OW32}, P_{OW31}	- Outerwall Pressures		

Figure 3-7
Instrumentation Transducer Locations Cross-Sectional View of 1/30 Scale Model

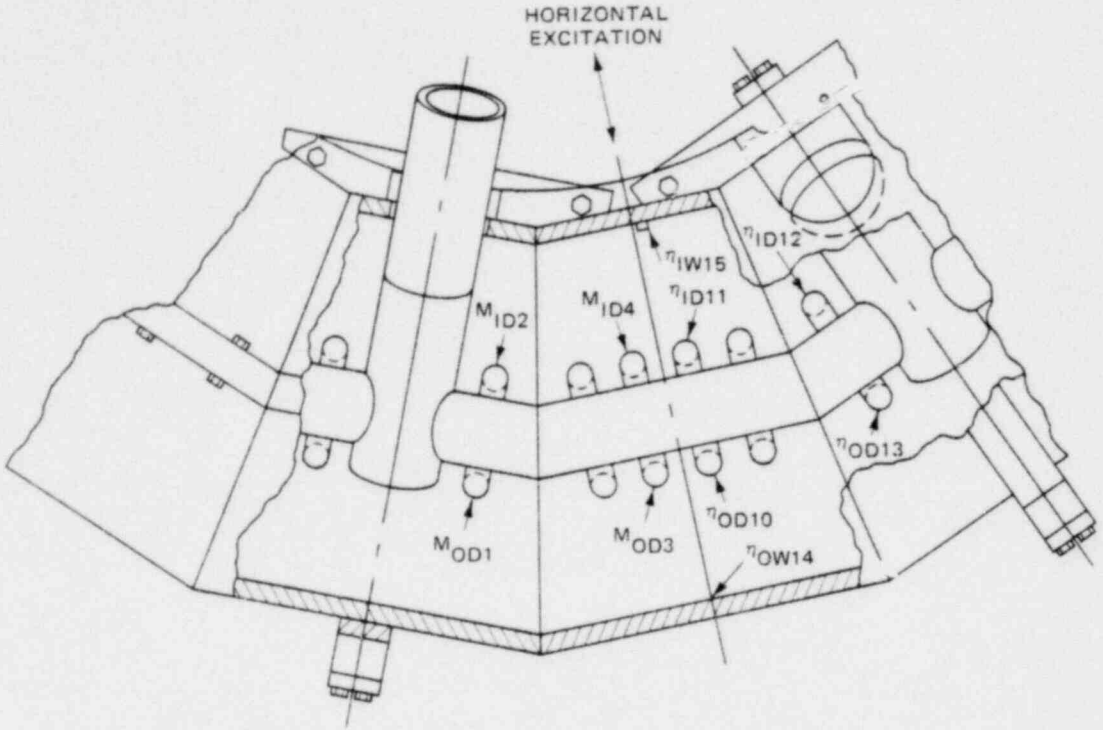

Figure 3-8
Instrumentation Transducer Locations Plan View of 1/30 Scale Model

Table 3-2

TAPE RECORDER CHANNEL ASSIGNMENT FOR DATA RUN

Tape Recorder Channel	Transducer Signal Identification	Symbol
1	Horizontal Table Acceleration	a_{1H}
2	Vertical Table Acceleration	a_{1V}
3	Horizontal Table Displacement	X_{1H}
4	Vertical Table Displacement	X_{1V}
5	Horizontal Tank Acceleration	a_{2H}
6	Vertical Tank Acceleration	a_{2V}
7	Outer Wall Pressure	p_{OW32}
8	Inner Wall Pressure	p_{IW30}
9	Outer Downcomer Moment	M_{OD3}
10	Outer Wall Wave Height	η_{OW14}
11	Outer Downcomer Wave Height	η_{OD10}
12	Inner Wall Wave Height	η_{IW15}
13	Horizontal Command Displacement	X_{CH}
14	Vertical Command Acceleration	a_{CV}

Table 3-3

TAPE RECORDER CHANNEL ASSIGNMENT FOR REPEATED DATA RUN

Tape Recorder Channel	Transducer Signal Identification	Symbol
1	Horizontal Table Acceleration	a_{1H}
2	Vertical Table Acceleration	a_{1V}
3	Horizontal Table Displacement	X_{1H}
4	Vertical Table Displacement	X_{1V}
5	Outer Wall Pressure	P_{OW31}
6	Outer Downcomer Moment	M_{OD1}
7	Inner Downcomer Moment	M_{ID2}
8	Inner Downcomer Moment	M_{ID4}
9	Inner Downcomer Moment	M_{ID6}
10	Inner Downcomer Wave Height	η_{ID11}
11	Inner Downcomer Wave Height	η_{ID12}
12	Outer Downcomer Wave Height	η_{OD13}
13	Horizontal Command Displacement	X_{CH}
14	Vertical Command Acceleration	a_{CV}

3.2.1 Earthquake Simulation

A biaxial (horizontal and vertical) seismic simulator was used for the testing. Earthquake time histories were developed in accordance with criteria described in Appendix B. For each test run, horizontal and vertical command signals were initially recorded on the tape recorder and then reproduced to drive the biaxial simulator for a given test run. Control accelerations and displacements were measured directly from the table motions. For the test runs, control accelerations were fed directly to a response spectrum analyzer to verify that the computed test response spectrum matched the required response spectrum, in accordance with the criteria specified in Appendix B. A control and analysis diagram of equipment used for the experiments is shown in Figure 3-9.

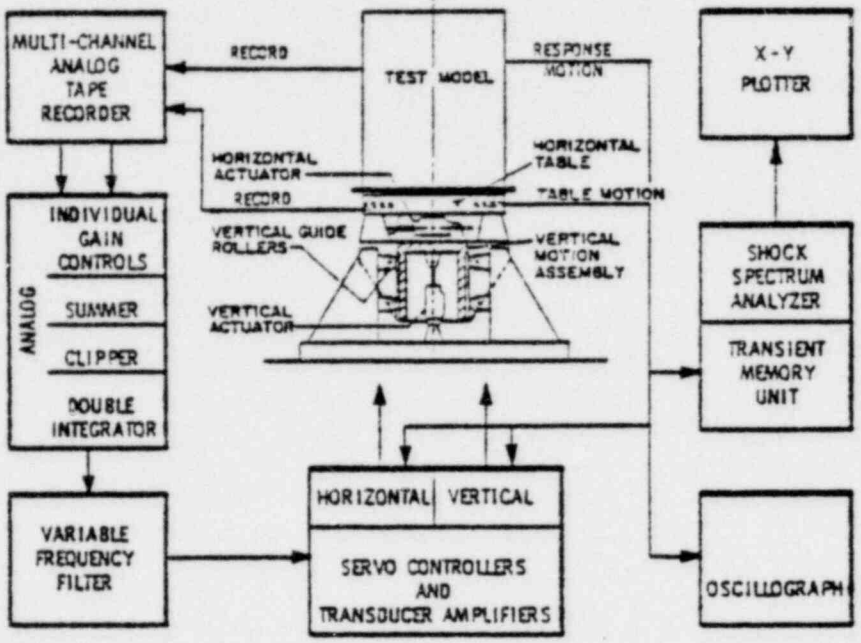

Figure 3-9
Control and Analysis Diagram for Biaxial Seismic Simulator

3.2.2 Pressure Transducers

Transducer locations were established during the preliminary tests using movable probes to obtain locations of maximum response. Two pressure transducers, P_{OW32} and P_{IW30}, were located 30 degrees below the torus horizontal diametrical plane, and the third, P_{OW31}, was located 45 degrees below this plane. Both P_{OW31} and P_{OW30} were mounted directly in the torus wall while P_{OW32} was mounted on a probe attached to the downcomer system. The effective point of measurement of the P_{OW32} transducer was 1/8-in. inside the torus wall.

3.2.3 Slosh Amplitude Transducers

The water slosh amplitude transducers consisted of two conductors separated by 1/4-in. The conductors located near downcomers were made of straight wire, while those at the torus wall were made of thin curved plates. As the sloshing water altered the conductance between the two wires, the measurements were taken with Wheatstone bridge arrangements and calibrated to produce slosh amplitude histories.

3.2.4 Moment Transducers

Downcomer moment transducers were made of thin aluminum strips instrumented with strain gauges, and inserted into the downcomers at the locations shown in Figure 3-8. The knee joint of these downcomers was left separated (although sealed from water) so that a lateral force on the downcomer would produce a strain gauge signal that was calibrated to the moment at the knee bend of the downcomers.

3.2.5 Calibration

System calibrations, which were performed for each group of data runs, were recorded on analog tape. Since the test runs required several days to perform, intermittent calibration checks on water slosh amplitude transducers were made. This was done by making visual observations of the slosh amplitude at the outer wall (η_{OW14}) while exciting the water at the first slosh mode (0.3 Hz) and comparing these observations to the voltage signal. Other transducers were considered sufficiently stable so no intermediate calibrations were conducted.

3.3 TEST CONDITIONS AND PROCEDURES

The following tests were conducted to gain the information necessary to correlate test model responses with those of the analytical model.

3.3.1 Adjustment of Support Conditions

The purpose of adjusting the support conditions is described in subsection 3.1. The analytical model (described in Section 4) predicts that only about 20% of the water in the torus acts as a rigid mass. However, the selected frequencies shown in Figure 3-2 were based on calculations that included a rigid mass assumption for the entire water mass. To verify the analytical prediction, the torus model support conditions were first adjusted to calculated empty torus frequencies. The torus was filled to the level scaled for the reference plant. The resulting measured frequencies were then compared with those predicted by the analytical model.

Both the flexible and medium support conditions were obtained in the above manner. The rigid condition was achieved by tapping 18 wooden shims between the tank bottom and base support plate while it was supported on the adjustable length support posts.

3.3.2 Low Frequency Sinusoidal Tests

A series of tests was conducted for fixed horizontal displacement harmonic excitation between 0-5 Hz to obtain transfer functions (ratio of output response to input response) of slosh parameters in the frequency range of interest. Slosh amplitude (η_{OW14}), pressure (P_{OW32}) and downcomer moments (M_{OD3}) were obtained by reading the transducer outputs on an oscilloscope during steady state conditions. Extremely low response times of water slosh precluded the possibility of acquiring data of this type under low frequency (5 Hz) sweep conditions.

Natural frequencies, mode shapes, and water modal damping were noted. The water modal damping was calculated from free decay records of the slosh amplitude. These data were recorded on analog tape, and motion pictures of natural modes under steady state conditions were taken.

3.3.3 High Frequency Sinusoidal Tests

The purpose of these tests was to determine the elastic and inertial properties of the model along each axis under harmonic excitation in the frequency range of 5 to 100 Hz. Tests were performed for each of the horizontal and vertical axes on each of the three different support configurations. Data were recorded from all transducers identified in Tables 3-2 and 3-3, while a constant amplitude table acceleration (approximately 0.1g peak) was swept in increasing frequency. Several of the response parameters were selected to demonstrate transfer functions in this frequency range.

3.3.4 Seismic Tests

Seismic tests were performed according to the matrix shown in Table 3-4. All flexible support configuration tests were performed first (runs 16 through 21), since this configuration had been used for developing the command histories at the SSE level. The signals for the other levels (OBE and 2 SSE) were achieved by lowering or raising the command input signals.

For the rigid support configuration, wood shims were installed and test runs 1 through 9 were performed. Then the wood shims were removed and the support posts adjusted for the medium support configuration of test runs 10 through 15.

Table 3-4

MARK I SIMULATED SEISMIC SLOSH TEST CONDITIONS AND RECORDED DATA

Test No.	Seismic Condition	Horizontal Acceleration Level (g)	Vertical Acceleration Level (g)	Excitation Direction	Data Recorded
A.	Rigid Support				
1	OBE	0.12		Horizontal (H)	22 Ch. Tape and Movie
2	OBE	0.08		Vertical (V)	22 Ch. Tape and Movie
3	OBE	0.12	0.08	H & V	22 Ch. Tape and Movie
4	SSE	0.24		H	22 Ch. Tape and Movie
5	SSE	0.16		V	22 Ch. Tape and Movie
6	SSE	0.24	0.16	H & V	22 Ch. Tape and Movie
7	2 SSE	0.50		H	22 Ch. Tape
8	2 SSE	0.32		V	22 Ch. Tape
9	2 SSE	0.50	0.32	H & V	22 Ch. Tape and Movie
B.	Medium Support				
10	OBE	0.12		H	22 Ch. Tape
11	OBE	0.08		V	22 Ch. Tape
12	OBE	0.12	0.08	H & V	22 Ch. Tape and Movie
13	SSE	0.24		H	22 Ch. Tape
14	SSE	0.16		V	22 Ch. Tape
15	SSE	0.24	0.16	H & V	22 Ch. Tape and Movie
C.	Flexible Support				
16	OBE	0.12		H	22 Ch. Tape
17	OBE	0.08		V	22 Ch. Tape
18	OBE	0.12	0.08	H & V	22 Ch. Tape and Movie
19	SSE	0.24		H	22 Ch. Tape
20	SSE	0.16		V	22 Ch. Tape
21	SSE	0.24	0.16	H & V	22 Ch. Tape and Movie

4. ANALYTICAL MODEL

The Mark I containment seismic slosh analytical model described herein was developed during the Mark III containment seismic slosh program. The analytical model for the annular tank of the Mark III suppression pool was modified to the Mark I torus geometry. The Mark I model includes the influence of dynamically modeled support frequencies on the slosh amplitudes and loads. Equations governing the slosh phenomena are presented below. Details regarding the derivation of these equations can be found in Reference 1.

4.1 APPLICATION OF THE ANALYTICAL MODEL TO THE TORUS GEOMETRY

To obtain analytical solutions for the seismic slosh response of a torus, an equivalent annular tank of equal volume and diameter was used. The torus and equivalent annular tank geometries are given in Figure 4-1. These tanks are geometrically related by the equivalent water level, h, given by:

$$h = \frac{d_i}{4} \text{ ARC COS } \left[(d_i - 2H_\ell)/d_i\right] - (\tfrac{1}{2} - H_\ell/d_i) \times \left[H_\ell (d_i - H_\ell)\right]^{\frac{1}{2}} \qquad (4.1)$$

The other geometric parameters are given for the inner tank radius, R_{in}, by $R_{in} = (D_m - d_i)/2$ and the outer tank radius, R_o, by $R_o = (D_m + d_i)/2$.

From the comparison of the two geometries in Figure 4-1, the equivalent annular tank appears to be a reasonable model for the torus with water level near half the tank diameter; i.e., $H_\ell/d_i \approx 0.5$. For this reason, a direct computation from the annular tank model was carried out for the slosh amplitudes and pressure loads, the difference being that a radial coordinate system with the origin at the water surface was used. Pressures along the torus wall can be determined from the annular model using the wall pressure at an equivalent angle from the torus centerline. Figure 4-1(b) shows the geometric relation between the torus and annular tank model for the location of the pressure equivalence.

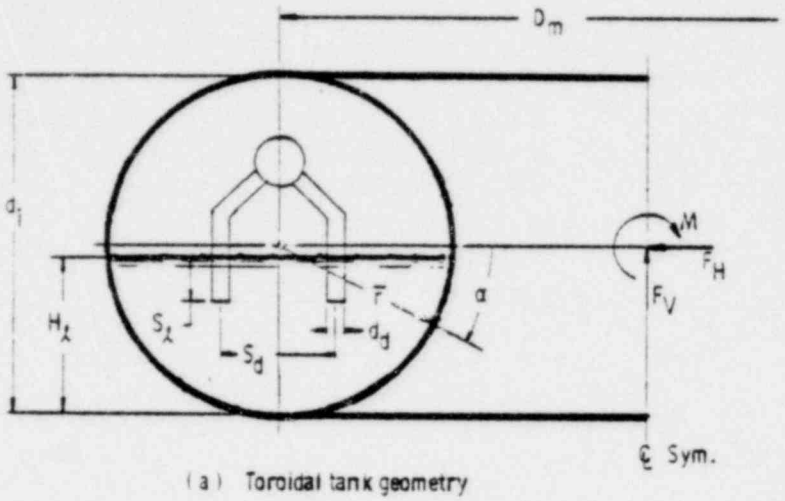

(a) Toroidal tank geometry

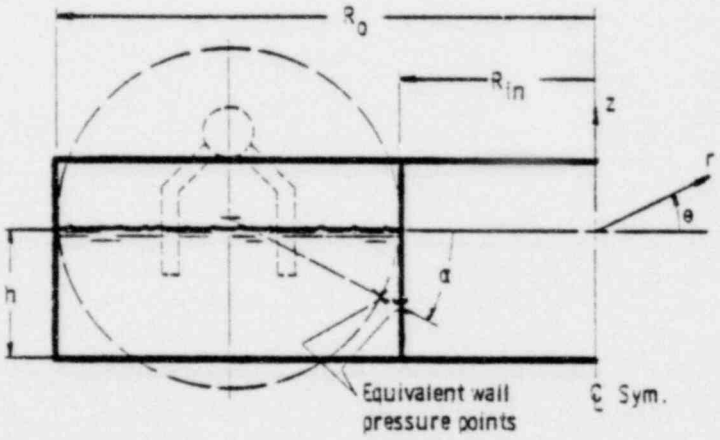

(b) Equivalent annular tank geometry

Figure 4-1
Toroidal and Equivalent Annular Tank Geometry

4.2 EQUIVALENT ANNULAR TANK MODEL

An equivalent mechanical model of the slosh caused by a random horizontal excitation of the annular tank can be given by a series of oscillating or slosh masses (m_i), supported by mechanical springs (k_i), that yield the corresponding slosh frequencies for a given tank geometry. The equivalent mechanical model of an elastically supported tank is shown in Figure 4-2. Symbols contained in the equations are defined in Appendix A. The oscillator masses and stiffness are given by the following equations:

$$\frac{m_i}{M_F} = \frac{A_i \left(\frac{2}{\xi_i} - kB_i\right) \tanh\left(\xi_i \frac{h}{R_o}\right)}{(1-k^2)\ \xi_i \left(\frac{h}{R_o}\right)} \tag{4.2}$$

and

$$\frac{k_i}{\pi \rho g R_o^2} = A_i \left(\frac{2}{\pi \xi_i} - kB_i\right)\left[\tanh\ \xi_i \frac{h}{R_o}\right]^2 \tag{4.3}$$

where

$$B_i = J_1(k\xi_i)\, Y_1'(\xi_i) - J_1'(\xi_i)\, Y_1(K\xi_i) \tag{4.4}$$

and

$$A_i = \frac{2\left(\frac{2}{\pi \xi_i} - kB_i\right)}{\left(\frac{2}{\pi \xi_i}\right)^2 (\xi_i^2 - 1) + B_i^2 (1 - k^2 \xi_i^2)} \tag{4.5}$$

The slosh eigenvalues ξ_i are zeros of the function:

$$F(k_1 \xi_i) = J_1'(\xi_i) Y_1'(k\xi_i) - J_1'(k\xi_i)\, Y_1'(\xi_i) \equiv 0 \tag{4.6}$$

where $k = R_{in}/R_o$. The total fluid mass is given by:

$$M_F = \pi \rho (R_o^2 - R_{in}^2) \times h \tag{4.7}$$

The rigid tank mass is given by:

$$m_N = M_T + M_F - \sum_{L=1}^{N-1} m_i \tag{4.8}$$

where M_T is the empty tank mass. The tank support stiffness is determined from the "rigid" liquid support frequency f_r by:

$$k_N = (M_T + M_F)\ (2\pi f_r)^2 \tag{4.9}$$

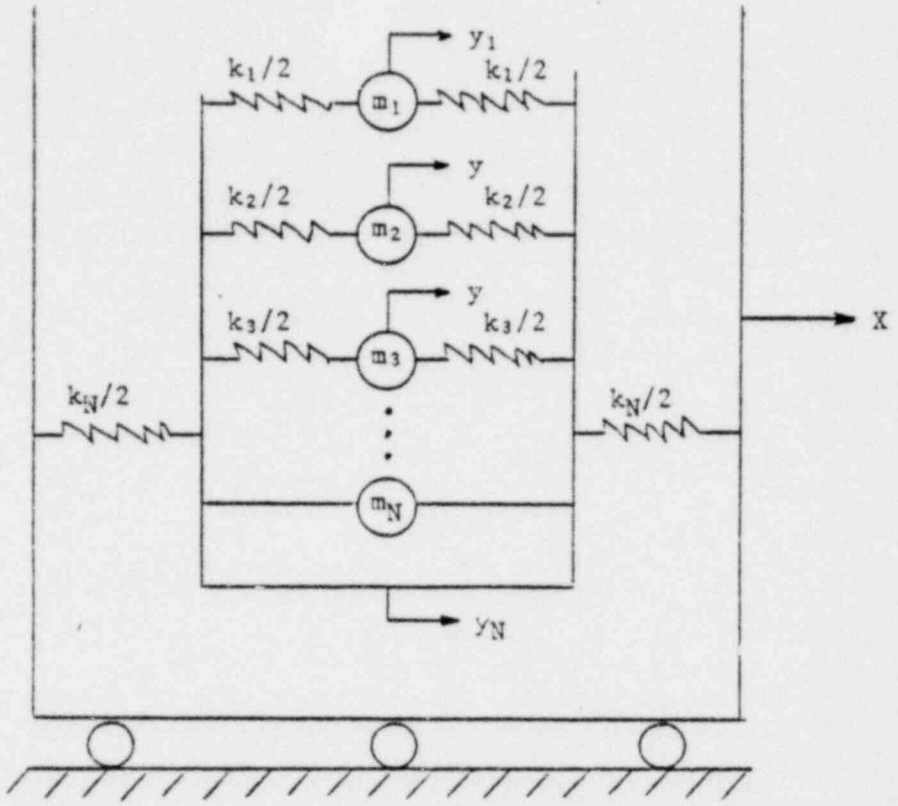

where:

y_i = displacement of the i^{th} slosh mass with respect to X, i=1, N-1.

y_N = displacement of tank with respect to X.

m_i = slosh masses, i=1, N-1.

m_N = rigid mass of liquid and tank.

k_i = liquid mass stiffness, i=1, N-1.

k_N = tank support stiffness.

X = base displacement.

Figure 4-2
Equivalent Mechanical Model of an Elastically Supported Tank

4.2.1 System Equations and Solution

The undamped equation of motion of the equivalent mechanical model is in matrix form:

$$\begin{bmatrix} m_1 & & & & \\ & m_2 & & & \\ & & m_3 & & \\ & & & \ddots & \\ & & & & m_N \end{bmatrix} \begin{Bmatrix} \ddot{y}_1 \\ \ddot{y}_2 \\ \ddot{y}_3 \\ \vdots \\ \ddot{y}_N \end{Bmatrix} + \begin{bmatrix} k_1 & & & & -k_1 \\ & k_2 & & & -k_2 \\ & & k_3 & & -k_3 \\ & & & \ddots & \vdots \\ -k_1 & -k_2 & -k_3 & \cdots & \sum_{L=1}^{N} k_i \end{bmatrix} \begin{Bmatrix} y_1 \\ y_2 \\ y_3 \\ \vdots \\ y_N \end{Bmatrix} = \begin{Bmatrix} -m_1 \\ -m_2 \\ -m_3 \\ \vdots \\ -m_N \end{Bmatrix} \ddot{X} \quad (4.10)$$

A solution to the equations of forced motion is most easily accomplished by an expansion of the equations in terms of the normal modes of free vibration. The matrix equations of motion can be written in the form:

$$M\ddot{y} + C\dot{y} + Ky = -M\ddot{X} \quad (4.11)$$

where a damping matrix considered to be proportional to the system mass or stiffness matrix is included. The system free vibration is determined from the homogeneous equations:

$$My + Ky = 0 \quad (4.12)$$

Assuming harmonic motion ($f(t) = e^{i\omega t}$) results in the linear eigenvalue problem:

$$\left[K - \lambda M\right] \left\{y\right\} = \left\{0\right\} \quad (4.13)$$

where $\lambda = \omega^2$. The normal mode eigenvectors are transformations from the generalized coordinates to the physical displacements:

$$\left\{y\right\} = \left[\phi\right] \left\{q\right\} \quad (4.14)$$

The eigenvectors are normalized such that they diagonalize the mass matrix to unity and the stiffness matrix to the square of the modal frequencies. Since the damping matrix was chosen to be proportional to the mass or stiffness, it can also be diagonalized, resulting in:

$$\left[I\right]\left\{\ddot{q}\right\} + \left[2\beta\omega_r\right]\left\{\dot{q}\right\} + \left[\omega_r^2\right]\left\{q\right\} = -\left[\phi\right]^T \left[M\right] \left\{\ddot{X}\right\} \quad (4.15)$$

The importance of normal mode expansion is apparent, in that the system equations are completely decoupled and appear as a series of damped single degree freedom oscillators forced at their base. For harmonic motion, the response of the r^{th} normal mode is:

$$q_r = \frac{\{\phi\}_r^T [M] \{I\} \ddot{X}}{(\omega_r^2 - \omega^2 + i\, 2\beta\omega_r\omega)} \tag{4.16}$$

By definition of the response spectrum (displacement):

$$S(\omega_r) = \frac{\ddot{X}}{(\omega_r^2 - \omega^2 + i\, 2\beta\omega_r\omega)} \tag{4.17}$$

the maximum modal response is:

$$q_r^{max} = \left| \phi_r^T \; M I \right| \; S(\omega_r) \tag{4.18}$$

and the maximum physical displacement of the i^{th} mass point due to the r^{th} normal mode is:

$$y_{ir}^{max} = \phi_{ir} \; q_r^{max} \tag{4.19}$$

The total displacement of the i^{th} mass due to all normal modes is found using the conventional square root of the sum of the squares (SRSS) method, thus:

$$y_i^{max} = \left[\sum_{r=1}^{N} (\phi_{ir} \; q_r)^2 \right]^{\frac{1}{2}} \tag{4.20}$$

4.2.2 Slosh Amplitudes, Pressures and Loads Calculation

From a series of approximate computations representative of Mark I plants, it was determined that only negligible coupling exists between the fluid slosh modes and the tank horizontal support mode. Thus, the response of the water modes with respect to base horizontal input are essentially the same as the response with respect to the tank walls. This allows a direct computation of the seismically induced slosh amplitudes, pressures, etc., as if the tank were mounted on the base directly.

Since the response y_i of the slosh masses are known with respect to the tank wall, the slosh amplitudes for each mode may be determined from:

$$\eta_i(r, \theta) = \left[\frac{2\, A_i}{\pi} \tanh\left(\xi_i \; \frac{h}{R_o}\right) \right] \frac{B_i(r)}{B_i(R_{in})} \; y_i \cos\theta \tag{4.21}$$

where

$$B_i(r) = J_1\left(\frac{r}{R_o}\xi_i\right) Y_1'(\xi_i) - J_1'(\xi_i) Y_1\left(\frac{r}{R_o}\xi_i\right) \tag{4.22}$$

The most probable slosh amplitude is determined by taking a SRSS of the modal contribution, i.e.:

$$\eta = \left[\sum_{i=1}^{NFM} \eta_i^2\right]^{\frac{1}{2}} \tag{4.23}$$

The slosh pressures are determined from:

$$\Delta p_{s_i} = -\rho g\left(\frac{2A_i}{\pi}\tanh\left(\xi_i \frac{h}{R_o}\right)\frac{B_i(r)}{B_i}\frac{\cosh\left[\xi_i \frac{z+h}{R_o}\right]}{\cosh \xi_i \frac{h}{R_o}}\right) y_i \cos\theta \tag{4.24}$$

where y_i are the displacements of the fluid masses with respect to the tank walls.

The most probable tank pressure is given by an SRSS combination of the individual contributions, i.e.:

$$\widetilde{\Delta p}(r,z,\theta) = \left[\sum_{i=1}^{NFM} (\Delta p_{s_i})^2\right]^{\frac{1}{2}} \tag{4.25}$$

The forces and moments acting at the center of the torus (see Figure 12) due to the slosh pressures are determined from:

$$F_{H_i} = \pi\left(\frac{R_o - R_i}{2}\right)\left\{\left(\frac{R_o + R_i}{2}\right)\int_{\alpha_i}^{\alpha_o} \bar{p}_i \cos\alpha \, d\alpha - \left(\frac{R_o - R_i}{2}\right)\int_{\alpha_i}^{\alpha_o} \bar{p}_i \cos^2\alpha \, d\alpha\right\} \tag{4.26}$$

and

$$M_i = -\pi\left(\frac{R_o - R_i}{2}\right)^2\left(\frac{R_o + R_i}{2}\right)\int_{\alpha_i}^{\alpha_o} \bar{p}_i \sin\alpha \, d\alpha \tag{4.27}$$

where $\alpha_i = \text{ARCSIN}(1 - 2H_i/d_i)$, $\alpha_o = \pi - \alpha_i$, $p_i = \bar{p}_i \cos\theta$, and $\bar{p}_i$ = pressure from the i^{th} slosh model. Note that the load contribution of each slosh mode response must be computed individually, and then the most probable load determined from an SRSS of the individual contributions.

The loads on the downcomers are computed based on the distribution of pressures and velocities existing in the undisturbed tank and the downcomers were assumed to be rigid for the load analysis. That is, no account of the elastic effects of the downcomers is included in the slosh model except to estimate the increased damping of the water due to the downcomers.

The slosh modes give rise to virtual mass forces and drag forces on the downcomer. The virtual mass forces and moments are given by:

$$F_{I_i} = C_m \rho \left(\frac{\pi d_d^2}{4}\right) \omega_i \int_{-S_\ell}^{0} \bar{V}_i \, dz \tag{4.28}$$

and

$$M_{I_i} = C_m \rho \left(\frac{\pi d_d^2}{4}\right) \omega_i \int_{-S_\ell}^{0} \bar{V}_i \cdot z \, d \, z \tag{4.29}$$

where C_m is the virtual mass force coefficient (C_m set to 2.0) and $\bar{V}_i$ is the maximum velocity component given by:

$$\bar{V}_i = \omega_i R_o y_i A_i \left[\frac{\cosh\left(\xi_i \frac{h+z}{R_o}\right)}{\cosh\left(\xi_i \frac{h}{R_o}\right)}\right]\left[\left(\frac{\partial B_i(r)}{\partial r}\right)^2 \cos^2\theta + \left(\frac{1}{r} B_i(r)\right)^2 \sin^2\theta\right]^{\frac{1}{2}} \tag{4.30}$$

The drag loads are given by:

$$F_{D_i} = \frac{1}{2} C_d d_d \rho \int_{-S_\ell}^{0} \bar{V}_i^2 \, dz \tag{4.31}$$

and

$$M_{D_i} = \frac{1}{2} C_d d_d \rho \int_{-S_\ell}^{0} \bar{V}_i^2 \cdot z \, dz \tag{4.32}$$

where C_D is the drag coefficient (C_D set to 1.0).

An SRSS combination of the above contributions yields the most probable load as given by:

$$F_D = \left[\sum_{i=1}^{NFM} F_{D_i}^2\right]^{\frac{1}{2}} \tag{4.33}$$

$$M_D = \left[\sum_{i=1}^{NFM} M_{D_i}^2\right]^{\frac{1}{2}} \tag{4.34}$$

The moment at a distance, e, above the water surface will be given by:

$$M_e = F_H \cdot (e) - M_W \tag{4.35}$$

where F_H is the horizontal force and M_W is the moment with respect to the water surface.

5. TEST RESULTS

5.1 COMPARISON OF ANALYTICAL AND EXPERIMENTAL RESULTS FOR THE 1/30 SCALE MODEL

Tables 5-1 through 5-3 give a comparison of analytical and experimental results for the 1/30 scale model slosh response to earthquake excitation. To determine any influence of support condition, the results are categorized according to the three different support conditions: rigid, medium and flexible, which represent arbitrarily selected frequencies. The analytical results are based on the use of the analytical model described in Section 4, plus the use of harmonic correction factors which are described in Section 5.5.2, and global correction factors that are described below.

A careful comparison of the data in Tables 5-1 through 5-3 indicates little or no influence of the support frequency on the slosh results. However, a difference between the analytical and experimental results can be noted for all cases. This discrepancy is attributed to the inherent inability of the equivalent annular model, including the harmonic correction factors, to provide an exact representation of seismic slosh in the toroidal configuration. The harmonic correction factors provide adjustment of the first, second and third mode responses from the analytical model for the slosh amplitude, pressure and downcomer moments for steady-state harmonic excitation response at frequencies less than 5 Hz. The majority of observed sloshing response occurred in the first and second slosh modes. An additional correction factor, termed the "global correction factor", is applied to results from the analytical model for prediction of seismic response. The global correction factors are developed from a statistical analysis of the data from the experimental and analytical results as described below.

Six experimental data points for each of the respective slosh amplitude, pressure and downcomer moment responses, which appear in Tables 5-1 through 5-3 (i.e., OBE and SSE levels for the three different support configurations), were used in a statistical analysis as shown in Table 5-4. Results given in Table 5-4 for the analytical model include the harmonic correction factors described in Section 5.5.2. For each parameter, a mean value, $\bar{X}$, and a standard deviation, σ, are given for each set of six ratios of experimental response to analytical value. The mean value, $\bar{X}$, is termed the global correction factor. A separate global correction factor was developed for each parameter of slosh amplitude, pressure and downcomer moment. These global correction factors are given in Table 5-4.

5.1.1 Application of One-Sided 95-95 Percent Statistical Tolerance Limit

The results predicted by the modified analytical model of Section 5.1 are conservative since the seismic response spectrum used in the seismic tests is an envelope of the individual response spectra for all the Mark I plants. The global correction factors are further modified for one-sided 95-95 percent statistical tolerance limit.

Global correction factors modified for a one-sided 95-95 percent statistical tolerance limit (STL) are calculated such that there is 95 percent confidence that at least 95 percent of the similar factors derived from a large series of similar experiments are less than that shown in Table 5-4.

Comparisons between the 1/30 scale analytical model and the experimental results are given in Tables 5-1 through 5-3 and Figures 5-1 through 5-3. In addition to experimental values for the OBE and SSE, values measured under the 2 SSE excitation conditions (i.e., Run 9 in Table 3-4) are included in the figures. The figures show the analytical values labeled "modified analytical model with 95-95 percent STL", while the experimental values are given as separate points. This line for each parameter contains the harmonic correction factor and the global correction factor modified for one-sided 95-95 percent STL. The procedure for application of the 95-95 percent STL to several of the parameters is as follows:

Company Proprietary

Equations for the other parameters are determined in a similar manner using the 95-95 percent STL in Table 5-4.

Table 5-1
COMPARISON OF SIMULATED EARTHQUAKE RESPONSES IN ANALYTICAL AND EXPERIMENTAL MODELS - RIGID SUPPORT
(GE Company Proprietary)

	Rigid Support			
	OBE*		SSE*	
Response Parameter	Analytical	Experimental	Analytical	Experimental

Company Proprietary

*Based on test response spectrum

Table 5-2
COMPARISON OF SIMULATED EARTHQUAKE RESPONSES IN ANALYTICAL AND EXPERIMENTAL MODELS - MEDIUM SUPPORT
(GE Company Proprietary)

	Medium Support			
	OBE*		SSE*	
Response Parameter	Analytical	Experimental	Analytical	Experimental

Company Proprietary

*Based on test response spectrum

Table 5-3

COMPARISON OF SIMULATED EARTHQUAKE RESPONSES IN ANALYTICAL AND EXPERIMENTAL MODELS - FLEXIBLE SUPPORT

(GE Company Proprietary)

	Flexible Support			
	OBE*		SSE*	
Response Parameter	Analytical	Experimental	Analytical	Experimental

Company Proprietary

*Based on test response spectrum

TABLE 5-4
DATA ANALYSIS FOR SLOSH RESPONSE PARAMETERS

(GE Company Proprietary)

Company Proprietary

Company Proprietary

HORIZONTAL DISPLACEMENT, X_{1H}-in

(a) Inner Wall

Company Proprietary

HORIZONTAL DISPLACEMENT, X_{1H}-in

(b) Inner Downcomer

Figure 5-1
Slosh Amplitude Response in Model Torus
(GE Company Proprietary)

Company Proprietary

HORIZONTAL DISPLACEMENT, X_{1H} -in

a. Inner wall

Company Proprietary

HORIZONTAL DISPLACEMENT, X_{1H} -in

b. Outer wall

Figure 5-2
Slosh Pressure Response In Model Torus
(GE Company Proprietary)

Company Proprietary

HORIZONTAL DISPLACEMENT, X_{1H}-in

Figure 5-3
Outer Downcomer Slosh Moment Response in Model
(GE Company Proprietary)

5.2 SEISMIC RESPONSE WITH RIGID SUPPORT

The excitation signals for the rigid support configuration are given in Figure 5-4. The acceleration and displacement histories are given with respect to the scaled time, which is equal to 1/30 times the full scale time. Similar time histories are obtained for the measured parameters for this support configuration in Figures 5-5, 5-6 and 5-7. Figure 5-8 shows slosh results for combined horizontal and vertical excitation. The pressure and moment responses of Figure 5-8 were obtained by low pass filtering the respective data below 5 Hz, to eliminate high frequency inertial components of response.

The nature of these responses indicates that:

a. Only horizontal motion excites water slosh. The slosh amplitude response is not influenced by the vertical excitation when subjected to combined horizontal and vertical motion.

b. The peak slosh response occurs near the end of the earthquake event with the principal response at that time in the second slosh mode. In the scale model, the slosh response peaks at about 5 seconds after the start of the earthquake, which is equivalent to approximately 27 seconds for the prototype. These measurements agree with the visual observations and movies.

c. Water motion at the outer downcomer includes a significant harmonic content. The peak wave amplitude at the inner wall exceeds that at the outer wall.

d. The pressure results are influenced by vertical excitation.

e. The torus horizontal acceleration (a_{2H}) is nearly equal to the ground horizontal acceleration (a_{1H}) at all times, which indicates good support rigidity along the horizontal axis. However, inherent vertical flexibility in the scale model was noted, in that the torus vertical acceleration (a_{2V}) is significantly larger than the ground vertical acceleration (a_{1V}).

f. Downcomer moment (M_{OD3}) appears to be principally an inertial mass response with slosh contribution of about 20 to 30 percent of the peak value. An effort was made to compensate M_{OD3} for structural mass by means of an external accelerometer; however, this correction was found difficult to achieve for the Plexiglas model.

Response spectra for all combined excitation runs for both axes are given in Figures 5-9 through 5-14. The horizontal test response spectra (TRS) generally indicate a significant conservatism in enveloping the required response spectra (RRS). The corresponding zero period accelerations (ZPA's) are also conservative. All horizontal response spectra indicate response at some resonance near 20 Hz, resulting from an inherent table mode in the simulator. Such a response is present at some similar frequency in any biaxial table and cannot be eliminated without extreme complexity. However, these system characteristics are not significant since one of the objectives of the test was to obtain data to verify the analytical model.

Company Proprietary

Figure 5-4
1/30 Scale SSE Excitations -- Rigid Support
(GE Company Proprietary)

Company Proprietary

Figure 5-5
1/30 Scale SSE Slosh Responses -- Rigid Support
Horizontal and Vertical (Test Run 6A)
(GE Company Proprietary)

Company Proprietary

Figure 5-6
1/30 Scale SSE Responses -- Rigid Support
Horizontal (Test Run 6A)
(GE Company Proprietary)

Company Proprietary

Figure 5-7
1/30 Scale SSE Responses -- Rigid Support
Vertical (Test Run 5A)
(GE Company Proprietary)

Company Proprietary

Figure 5-8
1/30 Scale SSE Filtered Responses -- Rigid Support
Horizontal and Vertical (Test Run 6A)
(GE Company Proprietary)

Company Proprietary

Figure 5-9
1/30 Scale OBE Horizontal Response Spectrum -- Rigid Support
(GE Company Proprietary)

Company Proprietary

Figure 5-10
1/30 Scale OBE Vertical Response Spectrum -- Rigid Support
(GE Company Proprietary)

Company Proprietary

Figure 5-11
1/30 Scale SSE Horizontal Response Spectrum -- Rigid Support
(GE Company Proprietary)

Company Proprietary

Figure 5-12
1/30 Scale SSE Vertical Response Spectrum -- Rigid Support
(GE Company Proprietary)

Company Proprietary

Figure 5-13
1/30 Scale 2 SSE Horizontal Response Spectrum -- Rigid Support
(GE Company Proprietary)

Company Proprietary

Figure 5-14
1/30 Scale 2 SSE Vertical Response Spectrum -- Rigid Support
(GE Company Proprietary)

Company Proprietary

Figure 5-15
1/30 Scale SSE Excitations -- Medium Support
(GE Company Proprietary)

5.3 SEISMIC RESPONSE WITH MEDIUM SUPPORT

The only significant variation noted for the medium support configuration was that the peak slosh responses are not affected significantly because of a lack of coupling of these modes with the support frequency. However, the slosh responses in Figures 5-16 through 5-19 appear to be slightly larger for the medium support condition than for the rigid support condition. This occurs because the horizontal displacement excitation is somewhat larger for the medium support than for the rigid support by nearly the same ratio, as can be seen by comparing Figures 5-15 and 5-4. Figure 5-19 is the combined results for horizontal and vertical excitation of Figure 5-16 with the pressure and moment responses produced by low pass filtering the respective data below 5 Hz to eliminate the high frequency inertial components of response. Response spectra for this configuration are given in Figures 5-20 through 5-23.

5.4 SEISMIC RESPONSE WITH FLEXIBLE SUPPORT

The excitation signals for the flexible support configuration are shown in Figure 5-24. The response time histories are stored on the analog tapes and are shown in Figures 5-25 through 5-28. Figure 5-28 shows the slosh results for the combined horizontal and vertical excitation of Figure 5-25 with the pressure and moment responses produced by low pass filtering the respective data below 5 Hz to eliminate the high frequency inertial components of response.

The following conclusions are noted for the flexible support configuration:

a. The torus horizontal and vertical accelerations (a_{2H} and a_{2V}) are somewhat more amplified for the flexible support case than for the medium support.

c. Significant vertical response occurs due to horizontal only excitation in Figure 5-26. This appears to result from cross-coupling due to inherent eccentricities in the system. The cross-coupling influence is also evident in the pressure traces.

Response spectra for the flexible configuration, combined horizontal and vertical excitation runs, are given in Figures 5-29 through 5-32.

Company Proprietary

Figure 5-16
1/30 Scale SSE Responses -- Medium Support
Horizontal and Vertical (Test Run 15A)
(GE Company Proprietary)

Company Proprietary

Figure 5-17
1/30 Scale SSE Responses -- Medium Support
Horizontal (Test Run 13A)
(GE Company Proprietary)

Company Proprietary

Figure 5-18
1/30 Scale SSE Responses -- Medium Support
Vertical (Test Run 14A)
(GE Company Proprietary)

Company Proprietary

Figure 5-19
1/30 Scale SSE Filtered Slosh Responses -- Medium Support
Horizontal and Vertical (Test Run 15A)
(GE Company Proprietary)

Company Proprietary

Figure 5-20
1/30 Scale OBE Horizontal Response Spectrum -- Medium Support
(GE Company Proprietary)

Company Proprietary

Figure 5-21
1/30 Scale OBE Vertical Response Spectrum -- Medium Support
(GE Company Proprietary)

Company Proprietary

Figure 5-22
1 30 Scale SSE Horizontal Response Spectrum -- Medium Support
(GE Company Proprietary)

Company Proprietary

Figure 5-23
1/20 Scale SSE Vertical Response Spect m -- Medium Support
(GE Company Proprietary)

Company Proprietary

Figure 5-24
1/30 Scale SSE Excitations -- Flexible Support
(GE Company Proprietary)

Company Proprietary

Figure 5-25
1/30 Scale SSE Responses -- Flexible Support
Horizontal and Vertical (Test Run 21A)
(GE Company Proprietary)

Company Proprietary

Figure 5-26
1/30 Scale SSE Responses -- Flexible Support
Horizontal (Test Run 19A)
(GE Company Proprietary)

Company Proprietary

Figure 5-27
1/30 Scale SSE Responses -- Flexible Support
Vertical (Test Run 20A)
(GE Company Proprietary)

Company Proprietary

Figure 5-28
1/30 Scale SSE Filtered Slosh Responses -- Flexible Support
Horizontal and Vertical (Test Run 21A)
(GE Company Proprietary)

Company Proprietary

Figure 5-29
1.30 Scale OBE Horizontal Response Spectrum -- Flexible Support
(GE Company Proprietary)

Company Proprietary

Figure 5-30
1/30 Scale OBE Vertical Response Spectrum -- Flexible Support
(GE Company Proprietary)

Company Proprietary

Figure 5-31
1/30 Scale SSE Horizontal Response Spectrum -- Flexible Support
(GE Company Proprietary)

Company Proprietary

Figure 5-32
1/30 Scale SSE Vertical Response Spectrum -- Flexible Support
(GE Company Proprietary)

5.5 RESULTS OF HARMONIC EXCITATION

5.5.1 Natural Modes

The seismic test system was subjected to harmonic excitation under steady-state conditions to define its dynamic characteristics. A summary of the theoretical and experimental natural mode data is given in Table 5-5. The given measured damping values represent averages because some variation with amplitude was observed. The measured natural frequencies for the slosh modes compare well with the theoretical results. However, transfer functions under steady-state harmonic excitation did not compare sufficiently well and adjustments for the discrepancies were made as discussed below.

5.5.2 Slosh Responses

A series of experiments to measure transfer functions under steady-state horizontal harmonic excitation was conducted for slosh amplitudes, pressures and downcomer moments. These experiments were conducted at low frequencies (0 to 5 Hz) and for constant table displacement amplitude. Data were taken for several different excitation conditions. A sample of typical transfer functions that resulted from such experiments is shown in Figure 5-33. The resonance modes at which significant responses occur are indicated on the figure. The second mode response is much more pronounced than the other two. These transfer functions are identical for all three support configurations.

Measured data acquired from these experiments were compared with those predicted by the analytical model described in Section 4. The majority of the low frequency slosh amplitude and pressure response during a seismic event is due to excitation of the first and second modes. The third and higher slosh modes are not significantly excited and contribute little to the response. To match these experimental data for the respective modes to the steady-state results predicted by the analytical model, it was necessary to incorporate the following harmonic correction factors for slosh amplitudes, pressures and downcomer moments in Equations 4.23, 4.25, and 4.34, respectively, for the first, second and third modes of predicted slosh response.

Table 5-8
SUMMARY OF NATURAL MODE DATA FOR MARK I TORUS MODEL
(GE Company Proprietary)

Company Proprietary

(GE Company Proprietary)

Company Proprietary

Figure 5-33
Slosh Transfer Functions for Water in Model Torus
(GE Company Proprietary)

The use of the correction factors eliminates the difference between the experimental data for steady-state harmonic excitation and analytical results for steady-state harmonic excitation which are apparently due to the representation of the toroidal tank by the equivalent annular geometry for frequencies below 5 Hz.

5.5.3 High Frequency Responses

Additional experiments were conducted at higher frequences (i.e., > 5 Hz) for both horizontal and vertical steady-state harmonic excitation. Transfer functions for tank acceleration (a_{2H} and a_{2V}), outer wall pressure p_{OW32}, and outer downcomer moment M_{OD3}, are shown in Figures 5-34 through 5-39. These responses demonstrate various degrees of tank and support flexibility at higher frequencies.

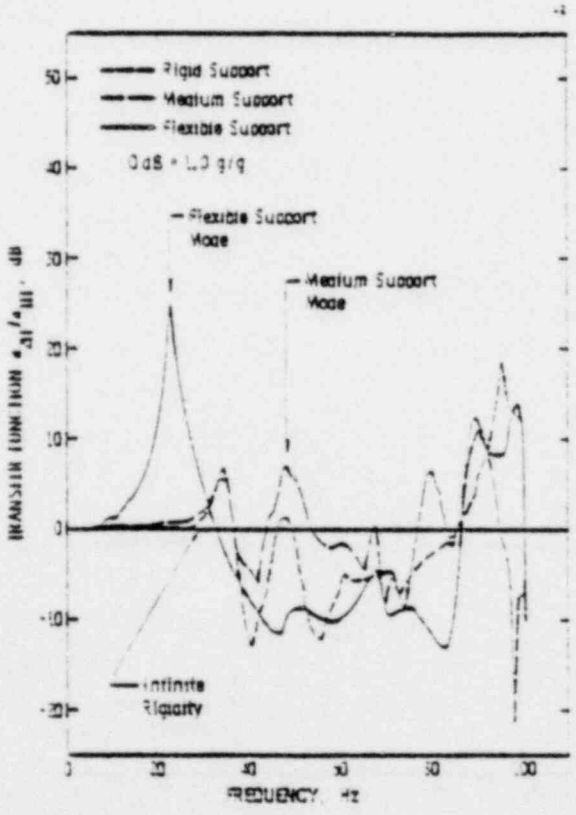

Figure 5-34
Tank Horizontal Acceleration Transfer Functions

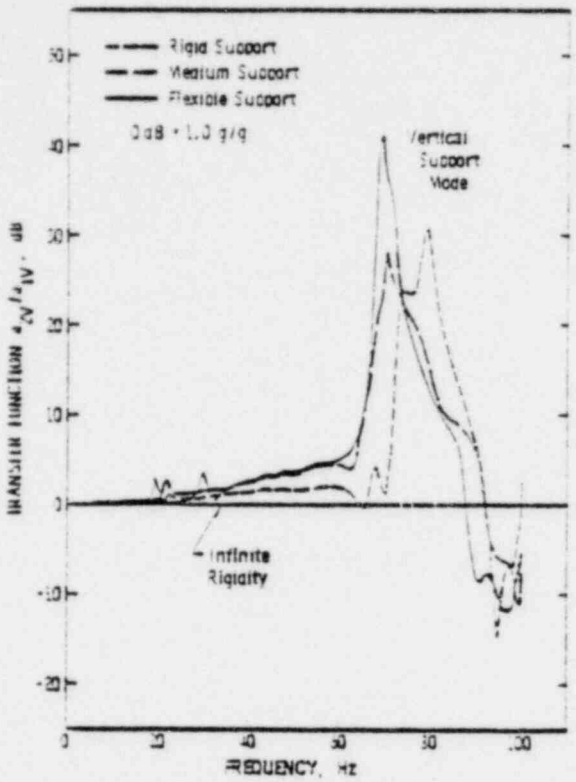

Figure 5-35
Tank Vertical Acceleration Transfer Functions

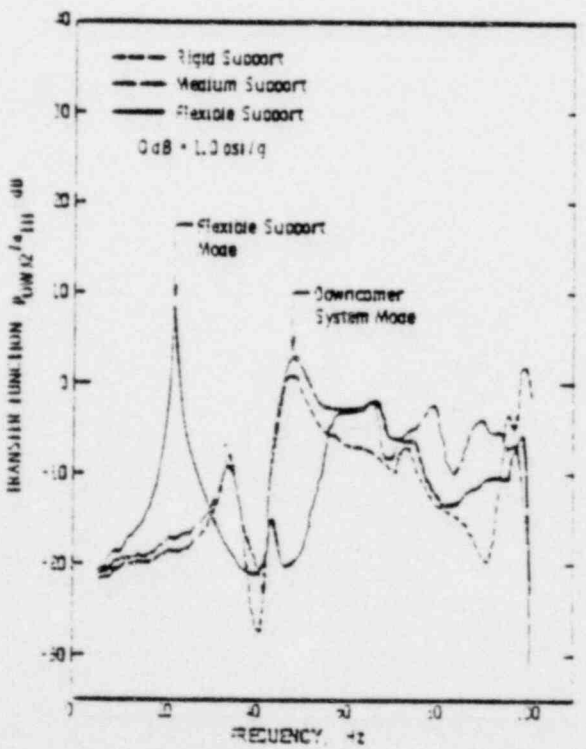

Figure 5-36
Outer Wall Pressure Horizontal Transfer Functions

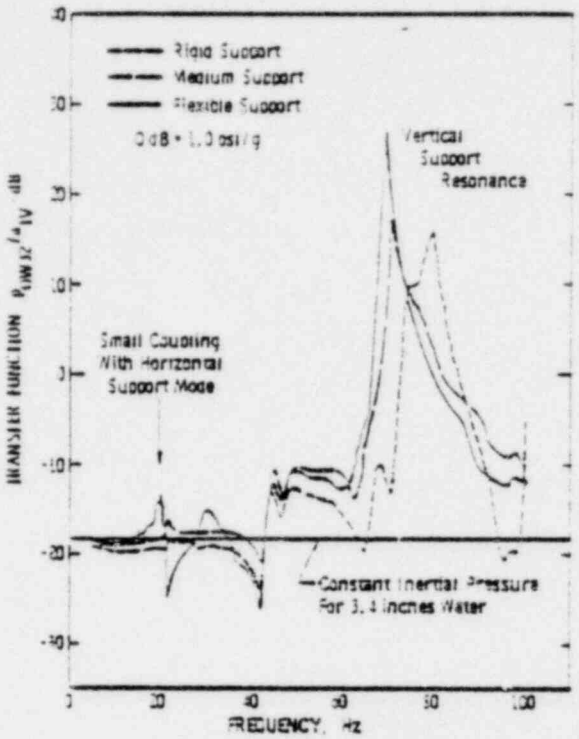

Figure 5-37
Outer Wall Pressure Vertical Transfer Functions

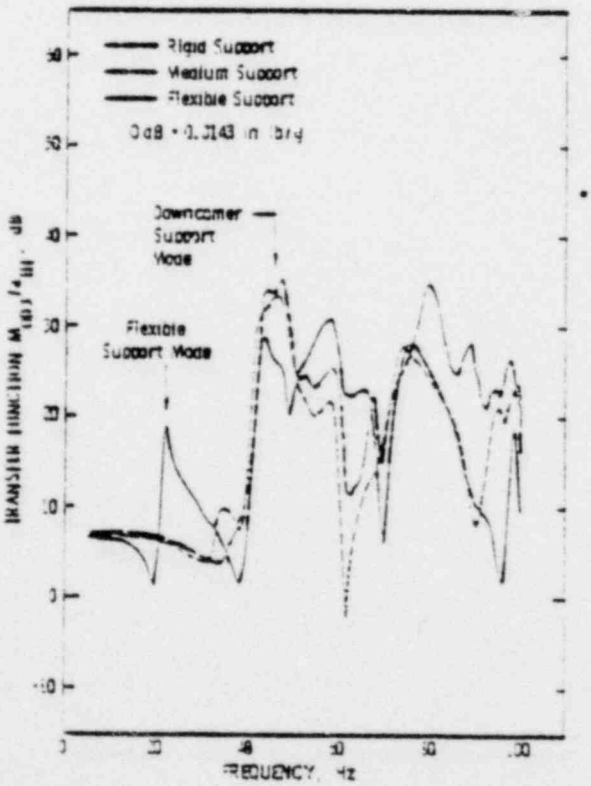

Figure 5-38
Outer Downcomer Moment Horizontal Transfer Functions

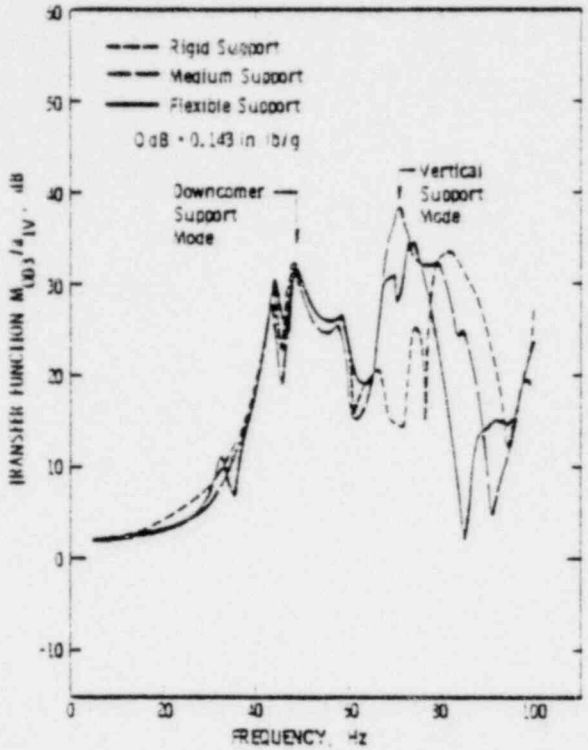

Figure 5-39
Outer Downcomer Moment Vertical Transfer Functions

6. REFERENCES

1. Reuter, F., and Petite, D., "Mark III Containment Seismic Slosh", GE Report NEDE-21069-P (Company Proprietary), General Electric Company, San Jose, California, November, 1975.

2. Abramson, H. N. (Editor), "The Dynamic Behavior of Liquids in Moving Containers", NASA-SP-106, Contract No. NASr-94(07), Southwest Research Institute, 1966.

APPENDIX A

GLOSSARY

SYMBOL	DEFINITION
d_d	Downcomer outer diameter
d_i	Toroidal tank cross section diameter
f_r	Tank with rigid liquid horizontal support frequency
g	Gravitational acceleration
h	Equivalent liquid height of annular tank model, ref. Eq. 4.1
i	Integer index or complex number $\sqrt{-1}$
k	Tank inner to outer radius ratio
k_i	Annular tank equivalent oscillator spring stiffness, ref. Eq. 4.3
k_N	Tank horizontal support stiffness, ref. Eq. 4.9
m_i	Annular tank equivalent oscillator slosh mass, ref. Eq. 4.2
m_N	Rigid mass of liquid and tank, ref. Eq. 4.8
q	Normal mode generalized degrees of freedom
q_r^{max}	Maximum response of the r^{th} mode, ref. Eq. 4.18
r	Radial coordinate or normal mode integer index
t	Downcomer thickness
y_i	Displacement of the i^{th} slosh mass with respect to X
$y_{i_r}^{max}$	Maximum displacement of the i^{th} slosh mass due to the r^{th} normal mode
y_i^{max}	Maximum displacement of the i^{th} slosh mass due to all normal mode responses

SYMBOL	DEFINITION
y_n	Displacement of the tank with respect to X
z	Vertical coordinate
A_i	i^{th} slosh mode amplitude coefficient, ref. Eq. 4.5
$B_i(r)$	i^{th} slosh mode radial shape functions
C	Proportional damping matrix
C_d	Drag coefficient
C_m	Virtual mass force coefficient
D_m	Torus mean diameter
F_{D_i}	Downcomer drag load, ref. Eq. 4.31
F_{H_i}	Torus horizontal load due to the i^{th} slosh mode, ref. Eq. 4.26
F_{I_i}	Downcomer virtual mass force due to the i^{th} slosh mode, ref. Eq. 4.28
H_e	Torus liquid level
I	Unit diagonal matrix
$J_1(z)$	Bessel function of the first kind order 1
$J_1'(z)$	Derivative of $J_1(z)$ with respect to z
K	Stiffness matrix
M	Mass matrix
M_e	Downcomer moment a distance e above liquid surface
M_i	Torus moment due to the i^{th} slosh mode, ref. Eq. 4.27
M_w	Downcomer moment at the liquid surface
M_{D_i}	Downcomer drag moment due to the i^{th} slosh mode, ref. Eq. 4.32

SYMBOL	DEFINITION
M_F	Total liquid mass
M_{I_i}	Downcomer virtual mass moment due to the i^{th} slosh mode, ref. Eq. 4.29
M_T	Empty tank mass
NFM	Number of slosh modes
R_{in}	Tank inner radius
R_o	Tank outer radius
S_d	Downcomer separation distance
S_ℓ	Downcomer submerge level
$S(\omega_r)$	Response spectrum displacement, ref. Eq. 4.17
$\bar{V}_i$	Maximum velocity component for the i^{th} slosh mode, ref. Eq. 4.30
X	Base displacement
$Y_1(z)$	Bessel function of the second kind, order 1
$Y_1'(z)$	Derivative of $Y_1(z)$ with respect to z
α	Angular position along toroidal tank wall
α_i	Angle to inner wall liquid surface
α_o	Angle to outer wall liquid surface
β	Critical damping ratio
$\eta_i(r,\theta)$	Wave height for the i^{th} slosh mode, ref. Eq. 4.21.
λ	Linear eigenvalue
ξ_i	i^{th} slosh eigenvalue, ref. Eq. 4.6
η	Total wave height due to all modal contributions

SYMBOL	DEFINITION
π	Constant 3.14159265.....
ρ	Liquid density
ϕ	Normal mode eigenvector
ϕ_{ir}	Contribution of the r^{th} normal mode to the i^{th} mass point
ψ_{η_i}	Harmonic correction factor for mode i of slosh amplitude
ψ_{M_i}	Harmonic correction factor for mode i of slosh moment
ψ_{p_i}	Harmonic correction factor for mode i of slosh pressure
ω	Normal mode circular frequency
Δp	Most probable tank pressure, ref. Eq. 4.25
$\widetilde{\Delta p}_{s_i}$	Pressure due to the i^{th} slosh mode, ref. Eq. 4.24
θ	Circumferential coordinate

APPENDIX B

MARK I TORUS SEISMIC RESPONSE SPECTRUM ENVELOPE

B.1 GENERAL DESCRIPTION

The seismic response spectrum, shown in Figure B-1, is a response spectrum obtained by geometrically enveloping the design response spectra for each of the Mark I containments listed in Table B-1. The design response spectra were obtained from the Mark I FSAR's.

B.2 SEISMIC REQUIREMENTS

The seismic response spectrum envelope shown in Figure B-1 was used for an overall representative seismic capability evaluation and testing of the Mark I plants listed in Table B-1. The seismic information shown in Figure B-1 was scaled according to dynamic scaling laws shown in Table 3-1.

The spectrum shown in Figure B-1 represents OBE response at critical damping ratios of 0.01 and 0.005. This spectrum was adjusted as follows to obtain SSE horizontal and OBE/SSE vertical responses:

SSE Horizontal	= 2 x OBE Horizontal (Figure B-1)
OBE Vertical	= 2/3 x OBE Horizontal (Figure B-1)
SSE Vertical	= 2 x OBE Vertical

The seismic input was based on an actual earthquake duration of 30 seconds.

Table B-1
MAXIMUM GROUND ACCELERATION COEFFICIENTS

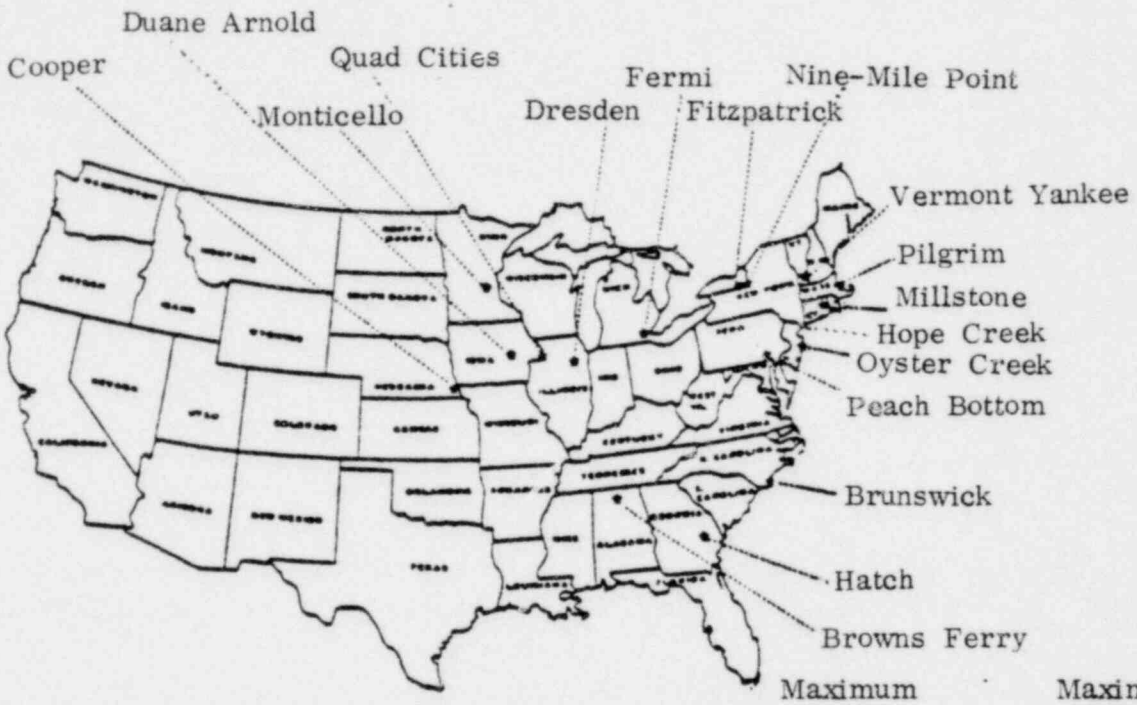

	Maximum Horizontal Acceleration (OBE/SSE)	Maximum Vertical Acceleration (OBE/SSE)
Brown's Ferry 1,2,3	0.10g/0.20g	0.07g/0.14g
Brunswick 1,2	0.08g/0.16g	0.06g/0.11g
Cooper	0.10g/0.20g	0.05g/0.10g
Dresden 2,3	0.10g/0.20g	0.07g/0.14g
Duane Arnold	0.06g/0.12g	0.04g/0.08g
Fermi 2	0.08g/0.16g	0.04g/0.08g
Fitzpatrick	0.08g/0.15g	0.06g/0.10g
Hatch 1,2	0.08g/0.15g	0.06g/0.10g
Millstone	0.07g/0.17g	0.05g/0.12g
Monticello	0.06g/0.12g	0.04g/0.08g
Nine Mile Point	0.06g/0.11g	0.05g/0.08g
Oyster Creek	0.11g/0.22g	0.08g/0.15g
Peach Bottom 2,3	0.05g/0.12g	0.033g/0.08g
Pilgrim	0.08g/0.15g	0.06g/0.10g
Quad Cities 1,2	0.12g/0.24g	0.08g/0.16g
Vermont Yankee	0.07g/0.14g	0.05g/0.09g
Hope Creek	0.10g/0.20g	0.07g/0.14g

* Based on FSARs

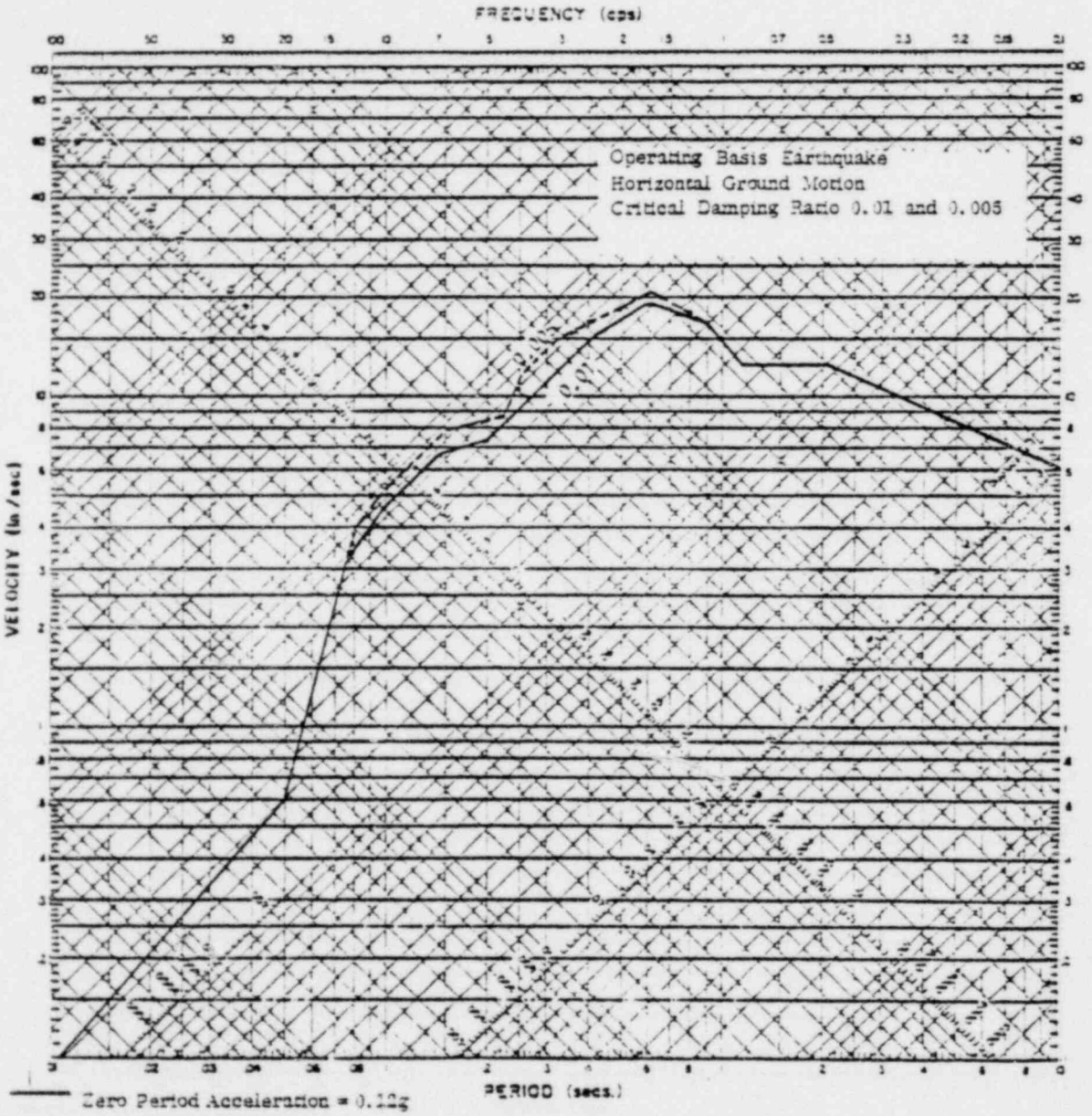

Figure B-1
Mark I Response Spectrum Envelopes